Computational Electrochemistry

DOI: 10.1002/anie.201206012

Construction of Pourbaix Diagrams for Ruthenium-Based Water-Oxidation Catalysts by Density Functional Theory**

Aleksandr V. Marenich, Abir Majumdar, Michelle Lenz, Christopher J. Cramer, and Donald G. Truhlar**

Efficient conversion of solar radiation into chemical fuels is important for the development of an energy economy less dependent on fossil fuels. One of the key reactions involved in the conversion of solar energy is the oxidation of water to molecular oxygen with the use of transition-metal catalysts, as highlighted previously.[1] We note a dramatic surge of activity in the search for novel transition-metal (in particular, ruthenium-based) molecular complexes able to catalyze effectively the oxidation of water to molecular oxygen.[2] A relevant task is the development of efficient schemes for the oxygenation of hydrocarbons with water as both the oxygen source and the solvent by using supported metal compounds as catalysts. For example, a recent experimental study[3] uncovered a number of highly efficient and selective catalytic oxygenation reactions of various hydrocarbons in water. The reactions were catalyzed by the complex $[Ru^{II}(tpa)(H_2O)_2]^{2+}$ (**1**), in which tpa is a tetradentate ligand (tpa = tris(2-pyridylmethyl)amine), through the formation of high-valency Ru=O intermediate species **1** by a series of proton-coupled electron-transfer reactions (Figure 1 a). The redox properties of **1** and its intermediates were also reported.[3] Another study[4] examined the synthesis and electrochemical properties of the complex $[Ru^{II}(db)(H_2O)]^{2+}$ (**2**) containing a pentadentate ligand (db = *N*,*N*-bis(2-pyridinylmethyl)-2,2′-bipyridine-6-methanamine; Figure 1 b). Complex **2** exhibited even higher catalytic activity for water oxidation than **1**.[4]

We present herein theoretical reduction potential–pH equilibrium diagrams (or Pourbaix diagrams[5]) for species **1** and **2** and their derivatives as based on density functional theory–continuum solvation calculations of the corresponding standard reduction potentials in aqueous solution (at pH 0) and the pK_a values corresponding to the deprotonation of one or more ligating water molecules in the first coordination shell. The goal of this study was to gain a better understanding of the electrochemistry of these compounds through the use of a specific computational protocol and to demonstrate that the higher levels of accuracy obtained in this way permit us not only to verify and complement existing experimental data, but also to identify and correct errors when they occur. Furthermore, the computational protocol established in the present study for predicting the reduction potentials of **1** and **2** will be of use for future studies involving other coordination compound catalysts in solution. We have also predicted the standard reduction potential of the bare $Ru^{3+} \mid Ru^{2+}$ couple in aqueous solution and the corresponding Pourbaix diagram, and have thus improved the results of our previous theoretical study of the aqueous $Ru^{3+} \mid Ru^{2+}$ reduction potential.[6]

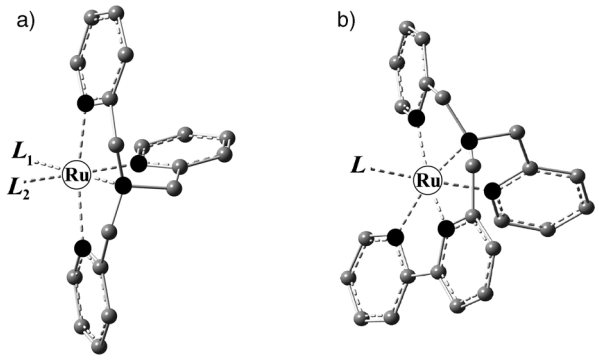

Figure 1. Molecular structures of a) the $[Ru(tpa)L_1L_2]^{q+}$ complex and b) the $[Ru(db)L]^{q+}$ complex. Hydrogen atoms are not shown, carbon atoms are gray, and nitrogen atoms are black. The ligands L, L_1, and L_2 are H_2O, OH^-, or O^{2-}. The total charge $q+$ varies from 0 to 3+, and the formal oxidation state of Ru varies from +2 (II) to +6 (VI).

We considered the following half-reaction (O = oxidized reagent, R = reduced reagent, n_p = number of protons (H^+), n_e = number of electrons (e^-), aq = aqueous, g = gaseous):

$$O(aq) + n_p\,H^+(aq) + n_e\,e^-(g) \rightarrow R(aq) \quad (1)$$

The standard reduction (redox) potential of the $O \mid R$ couple was computed (in volts) relative to the standard hydrogen electrode (SHE)[7] as

$$E^o_{O|R} = \frac{G^o(O,aq) + n_p G^o(H^+,aq) + n_e G^o(e^-,g) - G^o(R,aq)}{n_e F} - E^o_{SHE} \quad (2)$$

where F is the Faraday constant equal to the unit charge e, the quantities G^o are the standard-state Gibbs free energies of the corresponding species in electron volts (eV), and E^o_{SHE} is the absolute reference potential of the SHE equal to 4.28 V.[8] We

[*] A. V. Marenich, A. Majumdar, M. Lenz, Prof. C. J. Cramer, Prof. D. G. Truhlar
Department of Chemistry, Chemical Theory Center, and Supercomputing Institute, University of Minnesota
207 Pleasant Street SE, Minneapolis, MN 55455-0431 (USA)
E-mail: cramer@umn.edu
truhlar@umn.edu

[**] This research was supported in part by the U.S. Army Research Laboratory (W911NF09-100377), by the National Science Foundation (CHE09-56776 and CHE09-52054), by the Air Force Office of Scientific Research by grant no. FA9550-11-1-0078, and by an MSI Undergraduate Internship to M.L.

Supporting information for this article is available on the WWW under http://dx.doi.org/10.1002/anie.201206012.

also used the following other reference values: $G^{o}(e^{-},g) = 0.00\,eV$ and $G^{o}(H^{+},aq) = -11.72\,eV$ (see the Supporting Information for how these values were obtained). One advantage of using these reference data is that the contribution of the surface potential[9] need not be estimated.

All reduction potentials and pK_a values were calculated for standard conditions (298 K, ionic and neutral solutes at 1M, ideal gases at a partial pressure of 1 bar), as denoted by a small circle superscript.

The quantities $G^{o}(X, aq)$ ($X = O$ and R) were determined by a quantum-mechanical calculation:

$$G^{o}(X,aq) = E(X,g) + \varepsilon_{ZPE}(X,g) + G^{o}_{298K}(X,g) + \Delta G^{o}_{S}(X) \quad (3)$$

The first term on the right-hand side of Equation (3) is the electronic energy (including nuclear repulsion), the second term is the zero-point vibrational energy, and the third term is the thermal contribution to the Gibbs free energy for compound X in the gas phase. The last term in Equation (3) is the solvation free energy of X as defined as the free energy of transfer of the solute from the gas phase at a solute partial pressure of 1 bar to a 1M aqueous solution at 298 K.

We used two new density functionals, M11-L[10] and M11,[11] and the SMD[12] implicit solvation model (the SMD model was chosen because it gives mean unsigned errors in the absolute solvation free energies of ions of approximately 4 kcal mol^{-1}, as compared to approximately 7–12 kcal mol^{-1} with PCM and COSMO-type models[12]). The electronic energy and vibrational frequencies for all studied species (except H^+ and e^-) were calculated with the Gaussian 09 software[13] by using M11-L with the MG3S basis set at the gas-phase geometry optimized with the same density functional and basis set (the use of solution-phase vibrational frequencies would be expected to cause only a small change[14]). The notation MG3S denotes the 6-311 + G(2df,2p) basis set[15] on H, C, N, O along with the effective core potential ECP-28[16] on Ru (to replace 28 core electrons) and the ma-TZVP valence basis set on Ru. This last basis set was derived from the corresponding def2-TZVP basis set[17] according to a previously described procedure.[18] The solvation free energies $G^{o}_{S}(X)$ were calculated by using the SMD/M11-L/MG3S and SMD/M11/MG3S methods at fixed M11-L/MG3S geometries of the solute molecules as optimized in the gas phase. We considered multiple molecular conformations for each complex, and we included all low-energy conformations and spin states in a Boltzmann average. Further details are provided in the Supporting Information.

We computed the first, the second, and the third term of Equation (3) in the gas phase by using the M11-L/MG3S method, whereas the fourth term was computed by using either M11-L/MG3S or M11/MG3S. We chose M11-L and M11 because these new density functionals provide improved accuracy in comparison with other functionals against a broad database of energetic chemical properties.[10,11] The M11-L functional employs dual-range local exchange[10] and is a preferable choice for geometry optimization and frequency calculations because it has a smaller computational cost than M11, which employs range-separated-hybrid meta-generalized gradient approximation exchange.[11]

Table 1 shows the standard redox potentials for the studied half-reactions involving the Ru(tpa) and Ru(db) complexes (Figure 1) in comparison with available experimental data from Refs. [3] and [4], respectively. Table 1 also shows predicted values for the aqueous $Ru^{3+}|Ru^{2+}$ redox potential involving bare Ru^{2+} and Ru^{3+} cations, whereby the metal cations were modeled as the $[Ru(H_2O)_{18}]^{2+/3+}$ complex with 18 explicit water molecules (representing the first and second hydration shell) surrounded by continuum solvent. Table 2 shows the predicted pK_a values for several dissociation reactions of interest in comparison with experimental data from Refs. [3] and [4].

Pourbaix diagrams were constructed by using the Nernst equation[5] and computed values of the standard redox potential (at pH 0), and the corresponding pK_a values were

Table 1: Standard reduction potentials $E^{o}_{O|R}$.

Redox reaction	$E^{o}_{O\|R}$ [V] M11-L[a]	M11[b]	exp.[c]
Ru(tpa) complexes			
(1) $Ru^{III}(H_2O)(OH)^{2+} + H^+ + e^- \rightarrow Ru^{II}(H_2O)_2^{2+}$	1.04	0.94	0.85
(2) $Ru^{IV}(H_2O)(O)^{2+} + H^+ + e^- \rightarrow Ru^{III}(H_2O)(OH)^{2+}$	1.18	1.16	1.12
(3) $Ru^{V}(OH)(O)^{2+} + H^+ + e^- \rightarrow Ru^{IV}(H_2O)(O)^{2+}$	1.34	1.36	1.41
(4) $Ru^{III}(OH)_2^{+} + H^+ + e^- \rightarrow Ru^{II}(H_2O)(OH)^{+}$	0.66	0.59	0.85
(5) $Ru^{IV}(OH)(O)^{+} + H^+ + e^- \rightarrow Ru^{III}(OH)_2^{+}$	1.20	1.17	1.12
(6) $Ru^{V}(O)_2]^{+} + H^+ + e^- \rightarrow Ru^{IV}(OH)(O)^{+}$	1.45	1.45	1.41
(7) $Ru^{V}(O)_2^{+} + e^- \rightarrow Ru^{IV}(O)_2^{0}$	−0.44	0.02	0.98
(8) $Ru^{VI}(O)_2^{2+} + e^- \rightarrow Ru^{V}(O)_2^{+}$	1.13	1.29	1.22
MUE[d]	0.27	0.20	
Ru(db) complexes			
(9) $Ru^{III}(OH)^{2+} + H^+ + e^- \rightarrow Ru^{II}(H_2O)^{2+}$	1.11	0.99	0.92
(10) $Ru^{IV}(O)^{2+} + H^+ + e^- \rightarrow Ru^{III}(OH)^{2+}$	1.30	1.27	1.23
(11) $Ru^{III}(OH)^{2+} + e^- \rightarrow Ru^{II}(OH)^{+}$	0.27	0.34	0.35
(12) $Ru^{V}(O)^{3+} + e^- \rightarrow Ru^{IV}(O)^{2+}$	1.89	1.95	1.66
MUE[d]	0.14	0.10	
$Ru(H_2O)$ complexes			
(13) $Ru^{III}(H_2O)_{18}^{3+} + e^- \rightarrow Ru^{II}(H_2O)_{18}^{2+}$	0.19	0.20	0.23

[a] The SMD/M11 L/MG3S method was used for solvation calculations. [b] The SMD/M11/MG3S method was used for solvation calculations. [c] Experimental data for Ru(tpa) complexes were obtained from the Pourbaix diagram in Ref. [3] by extrapolating the original potentials (versus SCE) to pH 0 and applying the SCE→SHE conversion to them. The data for Ru(db) were obtained from Ref. [4] by extrapolating the potentials (versus SHE) to pH 0. The value for $Ru(H_2O)$ is from Ref. [6]. [d] Mean unsigned error relative to experimental reference values.

Table 2: Values of pK_a.

Redox reaction	pK_a [log units] M11-L[a]	M11[b]	exp.[c]
Ru(tpa) complexes			
(1) $Ru^{II}(H_2O)_2^{2+} \leftrightarrow Ru^{II}(H_2O)(OH)^{+} + H^{+}$	13.2	10.6	2.1
(2) $Ru^{II}(H_2O)(OH)^{+} \leftrightarrow Ru^{II}(OH)_2^{0} + H^{+}$	19.4	15.9	8.5
(3) $Ru^{III}(H_2O)_2^{3+} \leftrightarrow Ru^{III}(H_2O)(OH)^{2+} + H^{+}$	−2.1	1.0	–
(4) $Ru^{III}(H_2O)(OH)^{2+} \leftrightarrow Ru^{III}(OH)_2^{+} + H^{+}$	6.7	4.7	(2.1)
(5) $Ru^{IV}(H_2O)(O)^{2+} \leftrightarrow Ru^{IV}(OH)(O)^{+} + H^{+}$	7.0	4.8	(2.1)
(6) $Ru^{IV}(OH)(O)^{+} \leftrightarrow Ru^{IV}(O)_2^{0} + H^{+}$	32.0	24.2	(7.0)
(7) $Ru^{V}(OH)(O)^{2+} \leftrightarrow Ru^{V}(O)_2^{+} + H^{+}$	8.9	6.5	–
Ru(db) complexes			
(8) $Ru^{II}(H_2O)^{2+} \leftrightarrow Ru^{II}(OH)^{+} + H^{+}$	14.2	11.0	11.8
$Ru(H_2O)$ complexes			
(9) $Ru^{II}(H_2O)_{18}^{2+} \leftrightarrow Ru^{II}(OH)(H_2O)_{17}^{+} + H^{+}$	13.8	13.1	–
(10) $Ru^{III}(H_2O)_{18}^{3+} \leftrightarrow Ru^{III}(OH)(H_2O)_{17}^{2+} + H^{+}$	4.3	2.2	2.9

[a] The SMD/M11 L/MG3S method was used for solvation calculations. [b] The SMD/M11/MG3S method was used for solvation calculations. [c] The pK_a values for reactions (1) and (2) were measured by UV/Vis spectrophotometric titration;[3] the values given in parentheses were taken from the Pourbaix diagram in Ref. [3]. The reference pK_a value for Ru(db) complexes was measured by UV/Vis spectrophotometric titration,[4] and the reference pK_a value for $Ru(H_2O)$ complexes is explained in the text.

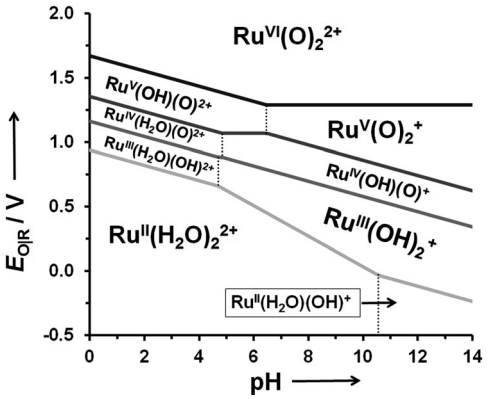

Figure 2. Pourbaix diagram for the Ru(tpa) complexes in aqueous solution. Vertical lines show the corresponding pK_a values.

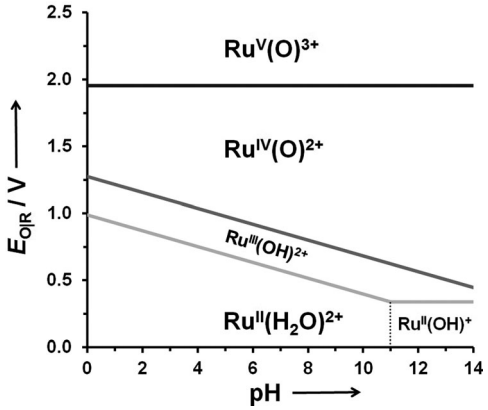

Figure 3. Pourbaix diagram for the Ru(db) complexes in aqueous solution. A vertical line shows the corresponding pK_a value.

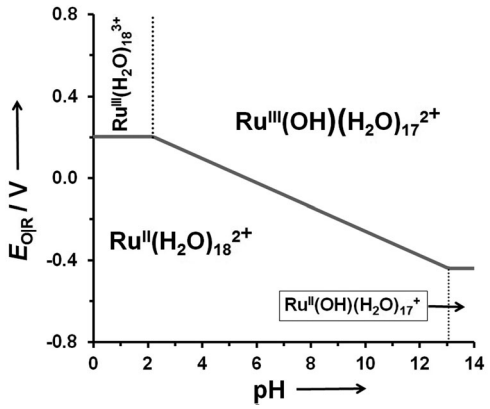

Figure 4. Pourbaix diagram for the $Ru(H_2O)$ complexes in aqueous solution. Vertical lines show the corresponding pK_a values.

predicted by using SMD/M11/MG3S for solvation calculations (Figures 2–4).

The theoretical standard redox potentials for the half-reactions of the Ru(tpa) and Ru(db) complexes as expressed by Equation (1), including the corresponding proton-coupled electron-transfer reactions ($n_p = 1$), agree reasonable closely (within 0.1–0.3 V) with the experimental data, with the exception of reaction (7) in Table 1, for which our prediction is in serious disagreement with the reference value of $E^{o}_{O|R}$ (0.98 V). The latter is derived from the value of approximately 0.74 V that corresponds to the $Ru^{IV}(O)_2/Ru^{V}(O)_2$ horizontal line in the experimental Pourbaix diagram of **1** in Ref. [3], as measured relative to the saturated-calomel-electrode (SCE) potential at room temperature.[3] (In this study, we applied an SCE→SHE conversion of 0.24 V.[7]) Our results suggest that the experimental assignment (i.e., the $Ru^{IV}(O)_2/Ru^{V}(O)_2$ horizontal line, which was based on only two measurements, see Figure 2 in Ref. [3]) should be revisited. Our confidence in the theoretical value over the experimental value was bolstered by the correct prediction of the value of $E^{o}_{O|R}$ for a similar reaction (1.13–1.29 versus 1.22 V for reaction (8); see Table 1) by our computational method. We also predicted quantitatively correct $E^{o}_{O|R}$ potentials (within 0.10–0.14 V on average) for reactions involving the Ru(db) complexes,[4] which are structurally similar to the Ru(tpa) complexes (Figure 1b).

The predicted pK_a value of **2**, which corresponds to a deprotonation of the H_2O ligand, is in reasonable agreement with the measured value[4] (Table 2), and the Pourbaix diagram of **2** (Figure 3) is supported by the experimental diagram.[4] However, the theory does not predict correctly the pK_a(1) and pK_a(2) values measured in another experimental study for **1**.[3] On the other hand, the experimental pK_a(1) value[3] of **1** (2.1 log units) is surprisingly small when compared to the analogous pK_a value[4] of **2** (11.8 log units). This large difference may indicate that an alternative assignment of p$K_a = 2.1$[3] merits consideration. For example, this pK_a value could be associated with a deprotonation of the H_2O ligand in $[Ru^{III}(tpa)(H_2O)_2]^{3+}$, for which a p$K_a$ value between −2.1 and 1.0 log units was predicted (Table 2). The experimental Pourbaix diagram[3] of **1** supposes that the pK_a

values corresponding to reactions (1), (4), and (5) in Table 2 should all be identical. Our theoretical protocols predict that the pK_a values of reactions (4) and (5) are similar but that they differ from that of reaction (1).

The standard reduction potential predicted in this study for the bare $Ru^{3+} \mid Ru^{2+}$ couple in aqueous solution (Table 1) by the use of mixed discrete–continuum solvation models (0.2 V) is in excellent agreement with the experimental reference values for the reaction $Ru^{3+}(aq) + e^- \rightarrow Ru^{2+}(aq)$ (0.23 ± 0.02 V;[6,19] 0.2487 V[19]). In our previous study,[6] we obtained an $E^o_{O|R}$ value for the $Ru^{3+} \mid Ru^{2+}$ couple in the range between -0.6 and $+1.0$ V by testing various density functionals (but not the newer M11, M11-L, or any other Minnesota density functional) combined with the SM6 implicit solvation model based on the generalized Born approximation and CM4 charges derived from Löwdin population analysis.[20] Löwdin population analysis may fail for molecules containing transition metals. In the present study, we found that the SMD model based on continuous charge density[12] (in conjunction with M11 and M11-L density functionals) is able to predict the studied properties more accurately. This model is much less sensitive to the choice of density functional, a characteristic we attribute to the treatment of the solute electronic density as a continuous distribution as opposed to its representation by partial atomic charges.

The Pourbaix diagram of the aqueous $Ru^{2+/3+}$ cations (Figure 4) with 18 water molecules added explicitly to represent the first and second hydration shell surrounded by continuum solvent is in close agreement with the experimental measurements[21] of $E_{Ru^{3+}|Ru^{2+}}$ as a function of the pH value, and in particular with the measured value of p$K_a = 2.90 \pm 0.05$ log units assigned to $[Ru(H_2O)_6]^{3+}$ in water and the value of $E^o_{O|R}$ =0.217 V (versus SHE) assigned to the $[Ru(H_2O)_6]^{3+/2+}$ couple; the value of $E_{Ru^{3+}|Ru^{2+}}$ is independent of the pH value at pH < 2.9.[21]

Our calculations were made possible by a significant advance in methodology. Moreover, theory has now improved to the point at which it can provide sufficiently reliable results to identify potential errors in experimental assignments. The resulting improved accuracy for transition-metal complexes opens new opportunities for the use of theory in the understanding and design of catalysts containing transition metals, especially when experimental values of the redox potentials and pK_a values are missing or uncertain owing to the difficulty of experimental studies on these complex systems.

Received: July 27, 2012
Revised: October 5, 2012
Published online: November 19, 2012

Keywords: density functional theory · electrochemistry · Pourbaix diagrams · ruthenium catalysis · solvation models

[1] a) J. L. Dempsey, A. J. Esswein, D. R. Manke, J. Rosenthal, J. D. Soper, D. G. Nocera, *Inorg. Chem.* **2005**, *44*, 6879 – 6892; b) H. Yamazaki, A. Shouji, M. Kajita, M. Yagi, *Coord. Chem. Rev.* **2010**, *254*, 2483 – 2491; c) A. Llobet, F. Meyer, DFG-Sonderpublikation in *Angew. Chem. Int. Ed.* **2011**, *50*, A30 – A33.

[2] a) J. C. Dobson, T. J. Meyer, *Inorg. Chem.* **1988**, *27*, 3283 – 3291; b) E. L. Lebeau, S. A. Adeyemi, T. J. Meyer, *Inorg. Chem.* **1998**, *37*, 6476 – 6484; c) M. H. Huynh, T. J. Meyer, *Chem. Rev.* **2007**, *107*, 5004 – 5064; d) J. Mola, E. Mas-Marza, X. Sala, I. Romero, M. Rodríguez, C. Viñas, T. Parella, A. Llobet, *Angew. Chem.* **2008**, *120*, 5914 – 5916; *Angew. Chem. Int. Ed.* **2008**, *47*, 5830 – 5832; e) X. Yang, M.-H. Baik, *J. Am. Chem. Soc.* **2008**, *130*, 16231 – 16240; f) F. Bozoglian, S. Romain, M. Z. Ertem, T. K. Todorova, C. Sens, J. Mola, M. Rodríguez, I. Romero, J. Benet-Buchholz, X. Fontrodona, C. J. Cramer, L. Gagliardi, A. Llobet, *J. Am. Chem. Soc.* **2009**, *131*, 15176 – 15187; g) Z. Chen, J. J. Concepcion, J. W. Jurss, T. J. Meyer, *J. Am. Chem. Soc.* **2009**, *131*, 15580 – 15581; h) Y. V. Geletii, Z. Huang, Y. Hou, D. G. Musaev, T. Lian, C. L. Hill, *J. Am. Chem. Soc.* **2009**, *131*, 7522; i) M.-K. Tsai, J. Rochford, D. E. Polyansky, T. Wada, K. Tanaka, E. Fujita, J. T. Muckerman, *Inorg. Chem.* **2009**, *48*, 4372 – 4383; j) X. Sala, M. Z. Ertem, L. Vigara, T. K. Todorova, W. Chen, R. C. Rocha, F. Aquilante, C. J. Cramer, L. Gagliardi, A. Llobet, *Angew. Chem.* **2010**, *122*, 7911 – 7913; *Angew. Chem. Int. Ed.* **2010**, *49*, 7745 – 7747; k) J. J. Concepcion, M.-K. Tsai, J. T. Muckerman, T. J. Meyer, *J. Am. Chem. Soc.* **2010**, *132*, 1545 – 1557; l) J. L. Boyer, D. E. Polyansky, D. J. Szalda, R. Zong, R. P. Thummel, E. Fujita, *Angew. Chem.* **2011**, *123*, 12808 – 12812; *Angew. Chem. Int. Ed.* **2011**, *50*, 12600 – 12604; m) S. Roeser, P. Farràs, F. Bozoglian, M. Martínez-Belmonte, J. Benet-Buchholz, A. Llobet, *ChemSusChem* **2011**, *4*, 197 – 207; n) L. Vigara, M. Z. Ertem, N. Planas, F. Bozoglian, N. Leidel, H. Dau, M. Haumann, L. Gagliardi, C. J. Cramer, A. Llobet, *Chem. Sci.* **2012**, *3*, 2576 – 2586; o) S. Maji, L. Vigara, F. Cottone, F. Bozoglian, J. Benet-Buchholz, A. Llobet, *Angew. Chem.* **2012**, *124*, 6069 – 6072; *Angew. Chem. Int. Ed.* **2012**, *51*, 5967 – 5970.

[3] Y. Hirai, T. Kojima, Y. Mizutani, Y. Shiota, K. Yoshizawa, S. Fukuzumi, *Angew. Chem.* **2008**, *120*, 5856 – 5860; *Angew. Chem. Int. Ed.* **2008**, *47*, 5772 – 5776.

[4] B. Radaram, J. A. Ivie, W. M. Singh, R. M. Grudzien, J. H. Reibenspies, C. E. Webster, X. Zhao, *Inorg. Chem.* **2011**, *50*, 10564 – 10571.

[5] C. H. Hamann, A. Hamnett, W. Vielstich, *Electrochemistry*, Wiley-VCH, Weinheim, **1998**, pp. 204 – 205.

[6] P. Jaque, A. V. Marenich, C. J. Cramer, D. G. Truhlar, *J. Phys. Chem. C* **2007**, *111*, 5783 – 5799.

[7] R. W. Ramette, *J. Chem. Educ.* **1987**, *64*, 885.

[8] a) A. Lewis, J. A. Bumpus, D. G. Truhlar, C. J. Cramer, *J. Chem. Educ.* **2004**, *81*, 596 – 604; b) Erratum: A. Lewis, J. A. Bumpus, D. G. Truhlar, C. J. Cramer, *J. Chem. Educ.* **2007**, *84*, 934.

[9] W. R. Fawcett, *Langmuir* **2008**, *24*, 9868 – 9875.

[10] R. Peverati, D. G. Truhlar, *J. Phys. Chem. Lett.* **2012**, *3*, 117 – 124.

[11] R. Peverati, D. G. Truhlar, *J. Phys. Chem. Lett.* **2011**, *2*, 2810 – 2817.

[12] A. V. Marenich, C. J. Cramer, D. G. Truhlar, *J. Phys. Chem. B* **2009**, *113*, 6378 – 6396.

[13] M. J. Frisch et al., Gaussian 09, Revision A.02; Gaussian, Inc., Wallingford, CT, **2009**.

[14] R. F. Ribeiro, A. V. Marenich, C. J. Cramer, D. G. Truhlar, *J. Phys. Chem. B* **2011**, *115*, 14556 – 14562.

[15] a) R. Krishnan, J. S. Binkley, R. Seeger, J. A. Pople, *J. Chem. Phys.* **1980**, *72*, 650 – 654; b) T. Clark, J. Chandrasekhar, G. W. Spitznagel, P. von R. Schleyer, *J. Comput. Chem.* **1983**, *4*, 294 – 301.

[16] a) Environmental Molecular Sciences Laboratory (EMSL) Basis Set Library at https://bse.pnl.gov/bse/portal (accessed July 13, **2012**); b) D. Andrae, U. Haeussermann, M. Dolg, H. Stoll, H. Preuss, *Theor. Chim. Acta* **1990**, *77*, 123 – 141.

[17] F. Weigend, R. Ahlrichs, *Phys. Chem. Chem. Phys.* **2005**, *7*, 3297 – 3305.

[18] J. Zheng, X. Xu, D. G. Truhlar, *Theor. Chem. Acc.* **2011**, *128*, 295 – 305.

[19] P. Vanýsek in *CRC Handbook of Chemistry and Physics*, 92nd ed. (**2011 – 2012**, internet version 2012; Ed.: W. M. Haynes), CRC, Boca Raton, FL, **2011**, pp. 5-80 – 5-89.
[20] C. P. Kelly, C. J. Cramer, D. G. Truhlar, *J. Chem. Theory Comput.* **2005**, *1*, 1133 – 1152, and references therein.
[21] a) W. Bottcher, G. M. Brown, N. Sutin, *Inorg. Chem.* **1979**, *18*, 1447 – 1451; b) D. T. Richens, *The Chemistry of Aqua Ions*, Wiley, New York, **1997**, p. 397.

